

CHAPTER 9

SCHIFF BASES DERIVED FROM PYRIDINE CARBONYL COMPOUNDS: SYNTHETIC MICROBIAL INDUCED CORROSION INHIBITOR FOR MILD STEEL IN MARINE ENVIRONMENT

This chapter deals with microbial induced corrosion (MIC) behaviour of four synthetic inhibitors derived from pyridine carbaldehyde and acetyl pyridine on mild steel in the artificial seawater medium, 1) *N*-hydroxy-1-(pyridin-2-yl)methanimine, NHP2M 2) *N*-hydroxy-1-(pyridin-3-yl)methanimine, NHP3M 3) (E)-2-(1-(2-phenylhydrazono)ethyl)pyridine, 2PHEP and 4) (E)-2-(1-triazylidinediethyl)pyridine, 2TAEP. It includes physicochemical and electrochemical techniques of these Schiff bases to monitor MIC.

Results and discussions

Identification of corrosion causing bacterium

Microorganisms inducing corrosion were selectively enriched by repeated subculturing in artificial seawater media. Streak plating techniques is used to obtain pure cultures of bacterial¹⁰¹. Individual isolates were re-tested to confirm the corrosion-inducing property of the strain. The cultures retaining the corrosion-inducing properties were systematically named and stored for further studies. The isolate labelled MICBT7 has shown significant metal deterioration activity on liquid media and agar medium. So, the strain MICBT7 was chosen as the active colony for corrosion enhancement in the present study. Table 9.1 gives the morphological characteristics of the selected bacterial isolate MICBT7.

❖ *Polymerase Chain Reaction (PCR)*

PCR-based rDNA amplification and sequencing²⁰¹ were used for the identification of bacterial isolate MICBT7. The whole genomic DNA of the isolated colony was isolated using the phenol-chloroform method. Quantity and purity of DNA isolate was accessed by 260/280 spectrophotometric analysis. Resulting DNA was

amplified using a pair of universal primers for rDNA in a PCR reaction. DNA amplification was confirmed by agarose gel electrophoresis and visualization in a UV transilluminator²⁰². Sequencing of the resulting culture showed the possibility of mixed culture of related bacteria in the isolate. Further steps are needed to separate and obtain pure cultures of the mixed isolate.

Table 9.1: Morphological characteristics of bacterial isolate MICBT7

Variable	Characteristics
Colony shape	Round
Colony size	Small
Edge	Entire
Surface	Smooth
Opacity	Opaque
Elevation	Raised
Colour	Light brown
Motility	Nonmotile
Cell shape	Rod
Cell size	Small

Weight loss measurements

Corrosion rate (v) and inhibition efficiency ($\eta\%$) of mild steel in control, biotic and inhibitor (100 ppm) systems for 21 days are summarized in Table 9.2. It was noted that the corrosion rate of 2.3620 mm/yr in the control system after 21 days, whereas, in the biotic system, it was 2.8207 mm/yr. The increase in corrosion rate for the latter may be due to forming a thick layer of biofilm on the metal surface²⁰³. It increased microbial induced corrosion rates of mild steel and changed cathodic or anodic reactions by creating an electrolytic environment. It has come to the knowledge that in the presence of Schiff base inhibitors, lower corrosion rates were identified, and a significant decrease in corrosion rate was noted with NHP3M compared to all other Schiff base inhibitors. On comparing the corrosion rate of the mild steel immersed in the control and biotic systems, all the four Schiff bases retarded the MIC rate of mild steel considerably. The decreasing order of inhibition efficiency of Schiff bases was NHP3M > 2PHEP >

NHP2M > 2TAEP. NHP3M attained a maximum inhibition efficiency of 60.3% at 100 ppm concentration. NHP3M and 2PHEP showed inhibition efficiency above 50%, while NHP2M and 2TAEP were achieved about 30% inhibition efficiency.

Appreciable efficiency of these Schiff bases may be ascribed to their molecular structure²⁰⁴. Presence of heteroatoms, aromatic ring systems, the possibility of forming intermolecular hydrogen bonding and intramolecular hydrogen bonding leads to effective binding of inhibitor molecules on the mild steel surface. Such a binding interaction may disturb the development of microbial growth. This hindrance to biofilm formation by adsorbing on the metal surface makes Schiff bases potent corrosion inhibitors. Inhibition efficiency of NHP2M and NHP3M can be attributed to hydrogen bonding⁹². As NHP3M molecules prefer intermolecular hydrogen bonding, the molecular assembly can sufficiently adsorb the mild steel surface. It may cause a noticeable decrease in the exposed surface area of the metal on which microorganisms can attack to form biofilm. NHP2M molecules interact with intramolecular hydrogen bonding. So NHP2M molecules can bind the metal surface separately, which means no interaction between the adsorbed molecules. It may cause the attack of microorganisms on the active sites of the metal surface, which are not blocking with inhibitors. So, the former reduces the MIC rate significantly than the latter.

It was reported that 2PHEP possessed a perfect planar geometry¹²⁹. The high inhibition efficiency of 2PHEP over 2TAEP can be ascribed to the presence of two aromatic rings in the former. It enhances pi-electron cloud and facilitates a strong adhesion to the metallic surface, which blocks active sites on the mild steel surface from the biofilm formation by microbes. Due to the absence of electron-rich centres other than azomethine linkage on 2TAEP behaved as a weak corrosion inhibitor.

From Table 9.2, it was apparent that all the four Schiff bases acted as inhibitors preventing biofilm formation and successfully reducing MIC rate. The corrosion rate of Schiff bases was increased to the maximum of about 1.6393 mm/year, which was lower than control (2.3620 mm/year) and biotic system (2.8207 mm/year). So, Schiff bases inhibited bacterial growth on the mild steel surface by adsorbing on the metal surface. It was proved that these Schiff bases could form a protective layer on the metal surface by the phenomenon of adsorption.

Table 9.2: Weight loss measurements of mild steel in control, biotic and Schiff base inhibitor systems

System	Corrosion rate (v) (mm/yr)	Inhibition efficiency ($\eta\%$)
Control	2.3620	-
Biotic	2.8207	-
NHP2M	1.6306	30.9%
NHP3M	0.9385	60.3%
2PHEP	1.1163	52.7%
2TAEP	1.6393	30.5%

Electrochemical impedance spectroscopy

Nyquist plots for the mild steel containing six biocorrosion systems for 21 days of incubation are exhibited in Fig. 9.1a). The corresponding impedance parameters such as charge transfer resistance (R_{ct}) and double-layer capacitance (C_{dl}) are shown in Table 9.3. Nyquist plot was seen in a semicircular shape for Schiff base inhibitor systems whereas, in the biotic systems, its curve was weakened at high-frequency values. This depression in the curve may occur due to the formation of a biofilm on the mild steel surface²⁰⁵. Similarly, Nyquist plot for the control system also showed depressed semicircle and lower R_{ct} ($40.79 \Omega \text{ cm}^2$) values than Schiff base inhibitor systems (Table 9.3), which recommends the localized corrosion on a metal surface. It has been realized that R_{ct} value was lower ($29.18 \Omega \text{ cm}^2$) for the biotic system than the control system, suggesting that microorganisms can form thick film on the mild steel surface and

enhance the corrosion process²⁰⁶. The higher R_{ct} values of the Schiff base inhibitor system were ascribed to the adsorption of inhibitor molecules and thus restriction of cathodic/anodic reaction on the mild steel surface.

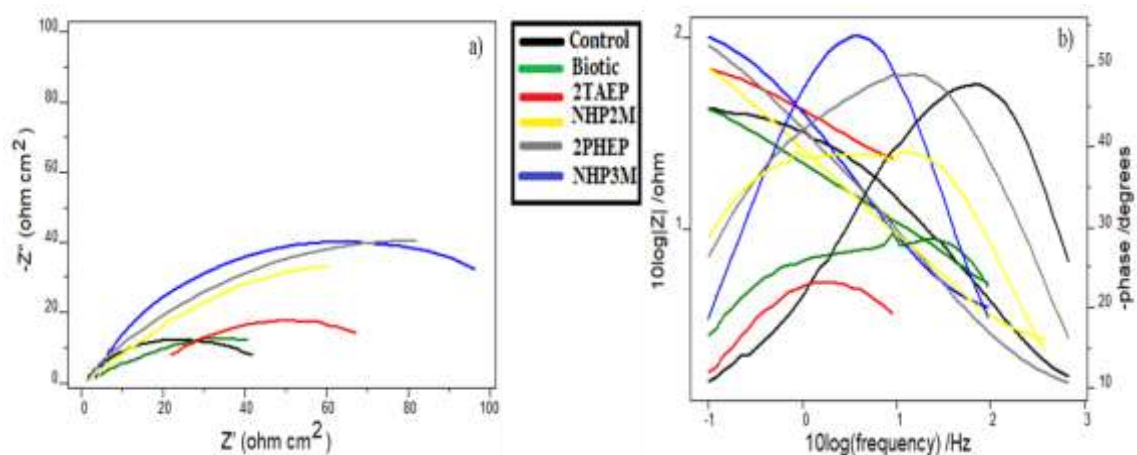


Fig. 9.1: a) Nyquist plots b) Bode plots of mild steel in control, biotic and Schiff base inhibitor systems

Table 9.3: Impedance parameters for mild steel in control, biotic and Schiff base inhibitor systems

System	C_{dl} (μFcm^{-2})	R_{ct} (Ω)	$\eta_{EIS}\%$
Control	0.006991	40.79	-
Biotic	0.009811	29.18	-
NHP2M	0.006447	62.25	34.47
NHP3M	0.004483	89.68	54.52
2PHEP	0.006021	80.82	49.52
2TAEP	0.006344	61.42	33.58

The lower C_{dl} values obtained for Schiff base inhibitor systems can be attributed to reducing local dielectric constant or increment in the electrical double layer thickness. This action may be due to the adsorption of these compounds at the metal–solution interface.

The Schiff base inhibitor systems NHP3M exhibited the highest corrosion inhibition efficiency, i.e. 54.52% at 100 ppm concentration. The decreasing order of inhibition efficiency of Schiff base inhibitor systems as follows: NHP3M > 2PHEP >

NHP2M > 2TAEP. This result was going along with data obtained in weight loss measurements.

Fig. 9.1 b) shows a Bode plot for the control, biotic and Schiff base inhibitor systems. It was observed that a sharp drop in $|Z|$ values at the low-frequency region for biotic and control systems, implying the accumulation of microorganisms and development of a biofilm on the mild steel surface²⁰⁷. In contrast, Bode plots for Schiff base inhibitor systems $|Z|$ values were tremendously higher at the low-frequency region even though there was no difference in the shapes of the Bode plots, inferring MIC inhibition capacity. The impedance spectra for all the systems were fitted with an equivalent circuit consisting of a solution resistance (R_s) in series with a parallel combination of charge transfer resistance (R_p) and double-layer capacitance (C_{dl}) as represented in Fig.1.7. The double-layer capacitance was replaced by a constant phase element because the roughness of a surface or biofilm deformity on the metal surface caused the dispersion effects. To summarize, electrochemical studies suggest the inhibition effect of the Schiff base inhibitors for the microorganism caused MIC of mild steel.

MIC inhibition of these Schiff base inhibitors can be explained as they appreciably reduced the contribution of microorganisms in the corrosion process. The studied Schiff base inhibitors minimized the growth of microorganisms and biofilm development by forming an adsorption layer that prevents the colonization of microbes on the metal surface. The protective shielding offered by Schiff bases may be attributed to adsorbed intermediates formed on the mild steel surface. Sini C V et al. investigated the inhibition efficiency of *N*-hydroxy-1-(pyridin-2-yl)methanimine and *N*-hydroxy-1-(pyridin-3-yl)methanimine on carbon steel corrosion in 1 M HCl and 0.5 M H₂SO₄ media⁹². Bincy M Paulson et al. studied the corrosion inhibition behaviour of (E)-2-(1-

(2-phenylhydrazono)ethyl)pyridine and (E)-2-(1-triazylidineethyl)pyridine on mild steel in acidic environments¹²⁹. Their findings recommended that these compounds acted as suitable metal corrosion inhibitors in acid solutions due to the chemical and physical adsorption of the compounds on the metal surface.

Potentiodynamic polarization studies

Fig. 9.2 reveals linear polarization and Tafel plots, and Table 9.4 presents corresponding potentiodynamic polarization parameters of mild steel in control, biotic and Schiff base inhibitor systems after 21 days of incubation. Fig. 9.2 b) displayed that the cathodic peak was changed to lower potential, and cathodic current density was increased ($260 \mu\text{A}/\text{cm}^2$) in the biotic system, suggesting the biofilm formation on the metal surface by microorganism.

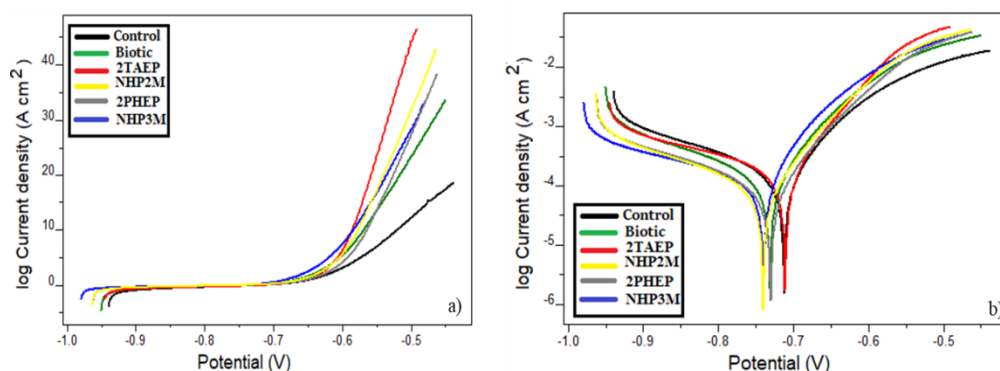


Fig. 9.2: a) Linear polarization and b) Tafel plots in control, biotic and Schiff base inhibitor systems

It has been observed that the corrosion current density for the control system ($208 \mu\text{A}/\text{cm}^2$) was lower when compared to the biotic system. Accumulation of microbes leads to high oxygen diffusion, which facilitates high i_{CORR} in the biotic system²⁰⁸. At the same time, in the presence of Schiff base inhibitors, i_{CORR} values were significantly smaller than control and biotic systems, which can be ascribed to absorption of these compounds on the metal surface.

Table 9.4: Potentiodynamic polarization parameters for control, biotic and Schiff base inhibitor systems

System	Tafel data				Polarization data		
	$-E_{\text{corr}}$ (mV)	i_{corr} ($\mu\text{A}/\text{cm}^2$)	b_a (mV/dec)	$-b_c$ (mV/dec)	$\eta_{\text{pol}}\%$	R_p (Ω)	$\eta_{R_p}\%$
Control	773.0	208	124	235	-	169.6	-
Biotic	761.8	260	150	256	-	158.2	-
NHP2M	736.3	121	77	224	41.82	295.4	42.58
NHP3M	714.6	100	121	244	51.92	374.2	54.67
2PHEP	746.3	115	95	217	44.71	310.0	45.29
2TAEP	759.7	125	96	234	39.90	281.2	39.68

It has been noted that the corrosion potential (E_{corr}) for the Schiff base inhibitor system was shifted to a positive potential indicating less susceptibility. This tendency revealed a better corrosion resistance on the metal surface. Herein, the change in corrosion potential was within 85 mV from the control system. So, these compounds were acted as a mixed-type inhibitor. Anodic and cathodic slope (b_a and b_c) values implied that Schiff base inhibitors affected cathodic and anodic branches of the Tafel plot and acted as a mixed type inhibitor. Previous studies reported that inhibition behaviour of these Schiff bases was mixed-type in acidic environments. From Table 9.4, it has been summarized that the polarization resistance (R_p) for the biotic system was dramatically lowered ($158.2 \Omega \text{ cm}^2$). In contrast, it was very much higher for Schiff bases and reached $374.2 \Omega \text{ cm}^2$ for NHP3M. The order of R_p values for Schiff bases was $\text{NHP3M} > \text{2PHEP} > \text{NHP2M} > \text{2TAEP}$. Hence, it was evident that NHP3M functioned as the best MIC inhibitor in the saline medium. Inhibition efficiency obtained from Tafel and linear polarization data was found to be in good agreement.

In vitro antibacterial effects of inhibitors

In vitro antibacterial effects of the Schiff base inhibitors NHP2M, NHP3M, 2PHEP and 2TAEP against *Escherichia coli* were performed at $500 \mu\text{g}/\text{disc}^{-1}$ in DMSO. Tetracycline was used as a standard antibiotic to verify the activity of Schiff base inhibitors. Table 9.5 and Fig. 9.3 exhibits the antibacterial effects of the Schiff base

inhibitors. Diameter of the zone of inhibition shown by tetracycline in *E. coli* is 20 mm. All the Schiff base inhibitors exhibited a zone of inhibition except NHP3M. 2TAEP showed a maximum zone of inhibition of about 19 mm. The order of antibacterial effect was $\text{NHP3M} < \text{NHP2M} < \text{2PHEP} < \text{2TAEP}$.

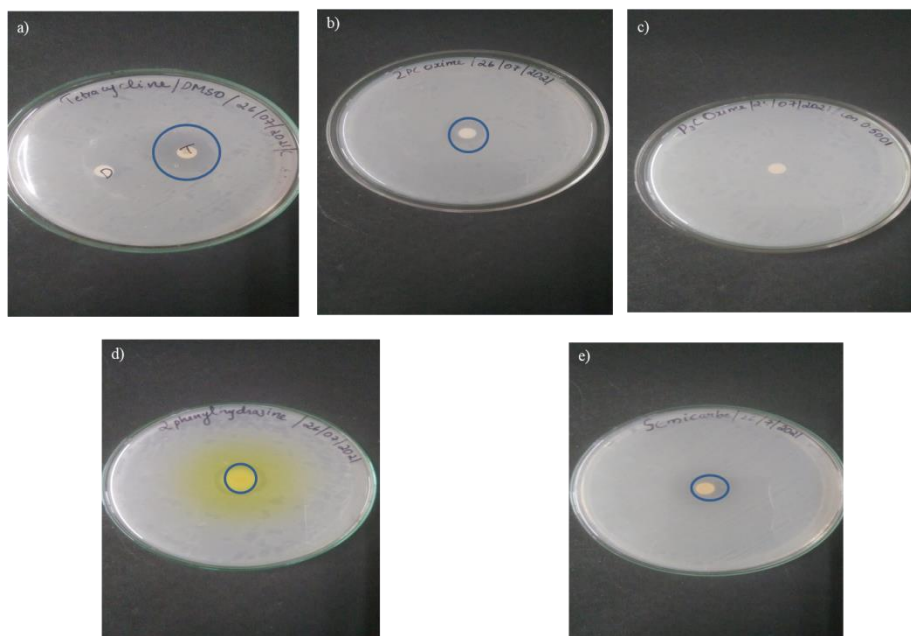


Fig. 9.3: Antibacterial effects of a) Tetracycline b) NHP2M c) NHP3M d) 2PHEP e) 2TAEP against *E. coli* at $500 \mu\text{gdisc}^{-1}$ in DMSO

Table 9.5: Antibacterial effects of the Schiff base inhibitors at $500 \mu\text{gdisc}^{-1}$ in DMSO against *Escherichia coli*

Inhibitor	Zone of inhibition (mm)
NHP2M	15
NHP3M	No zone of inhibition
2PHEP	18
2TAEP	19
Tetracycline	20

It has been noted that NHP3M was the inhibitor with the highest MIC inhibition efficiency. But it is not an antibacterial agent. So, the proposed mechanism of inhibition is that Schiff base molecules destabilize biofilm formation by adsorption of Schiff base molecules on the mild steel surface, not by killing the microorganism. 2TAEP was found to be the inhibitor with the comparatively highest antibacterial activity. But, it was not a suitable MIC inhibitor. In this case, the binding interaction of 2TAEP with the

metal surface was not sufficient to disturb the biofilm growth formed on the metal surface. This result revealed the relevance of these Schiff base inhibitors in inhibiting MIC rather than toxic and harmful antibacterial agents. So, the selected Schiff base inhibitors can be applied as MIC inhibitors for mild steel in the marine environment.

Mechanism of MIC inhibition

Mechanism of MIC inhibition by Schiff base inhibitors can be established by surface analysis, microscopic surface analysis and UV-Visible spectroscopy.

❖ *Surface analysis*

FTIR spectroscopy

FTIR spectroscopy of the corrosion products furnishes an idea about the interaction of Schiff base inhibitors on the mild steel exposed in the biotic medium. Fig. 9.4 gives the FTIR spectra of corrosion products obtained from the mild steel surface exposed to control, biotic and Schiff base inhibitor systems at the end of 21 days of the incubation period. The broad peak was observed at 3200–3400 cm^{-1} for NHP3M and 2PHEP systems due to -OH and -NH stretching vibrations of hydroxyl groups and aromatic amines deposited on the mild steel surface, respectively. The distinguishing peak observed for Schiff base inhibitor systems was at 1347 cm^{-1} , attributed to C-N stretching vibration. This stretching frequency confirmed the adsorption of the imine group on the mild steel surface. These intense peaks were absent in the spectrum of control and biotic systems.

These noticeable changes in the IR spectra give the mechanism of MIC inhibition by Schiff base molecules. The presence of Schiff base inhibitors as corrosion products on the mild steel surface may cause interaction of Schiff base molecules with the biofilm formed on the metal surface. Schiff base molecules may be locked on the biofilm and cause destabilization of biofilm. Schiff base inhibitors may act as destabilizing agents for

biofilm growth by adsorbing on the metal surface. FTIR revealed the role of Schiff base molecules in inhibiting microbially influenced corrosion.

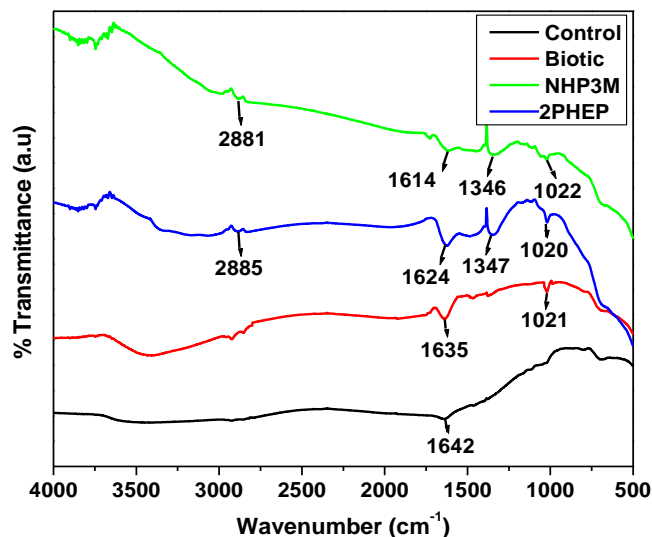


Fig. 9.4: FTIR spectra of corrosion products formed on mild steel surfaces of control, biotic and inhibitor systems

X-ray diffraction spectroscopy (XRD)

Fig. 9.5 shows the XRD spectra of the mild steel surface immersed in control, biotic and inhibitor systems after 21 days of incubation. High-intensity peaks observed in all systems at 44.7°, 65.1° and 82.3° indicated Fe (0) metal²⁰⁹. Peak at 35.1° in the control and biotic systems represented Fe₂O₃ formed as corrosion products²¹⁰. In the presence of Schiff base inhibitors, the intensity of peak at 35.1° was decreased due to the prevention of the bacterial biofilm formation on the mild steel surface. In the biotic system, another corrosion product FeO was detected at 42.7° with low intensity. Similarly, in the 2TAEP system, significantly lower intensity of iron oxide peak was observed, which indicated relatively lower inhibition efficiency of 2TAEP than all other inhibitor systems.

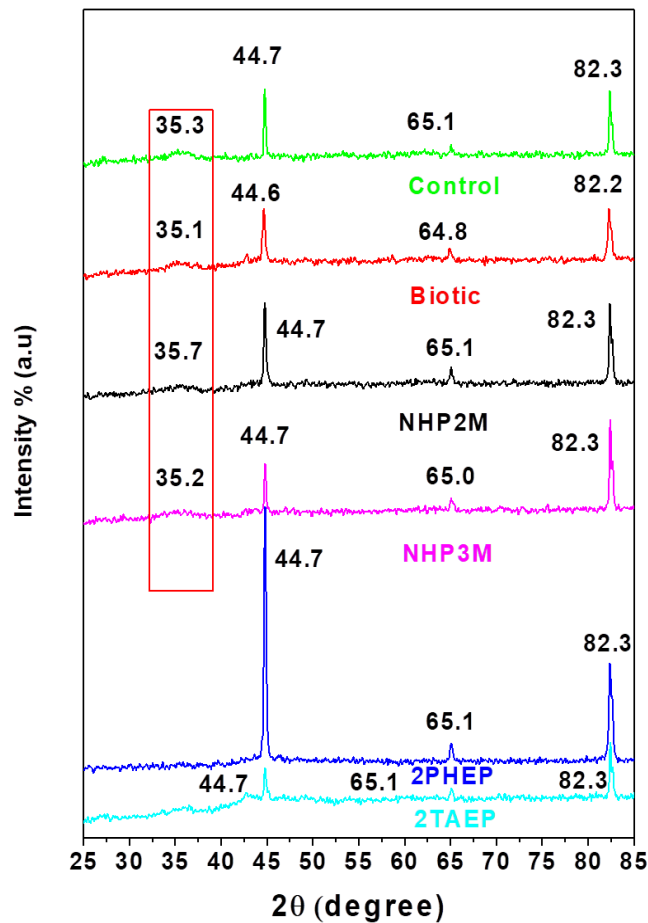


Fig. 9.5: XRD spectra of mild steel surface immersed in control, biotic and inhibitor systems

❖ *Microscopic surface analysis*

Optical microscopic images²¹¹ of the mild steel coupons exposed in control, biotic and inhibitor systems after 21 days are exhibited in Fig. 9.6. The more hydrated ferric oxide was present on the mild steel coupon exposed in the biotic medium than other metal coupons. It is established that the mild steel coupon exposed in the biotic medium has enhanced corrosion due to the stable and quick biofilm formation on the metal surface. Biofilm causes metal destruction gradually. In comparison, the mild steel coupon exposed in inhibitor systems like NHP3M has only little oxide content. Mild steel exposed in 2TAEP were found to be more corrosive compared to all other inhibitors. Mild steel coupons exposed in 2PHEP and NHP2M

were observed as a better MIC inhibitor than 2TAEP. Thus the capacity of inhibitor systems to prevent the MIC in the artificial sea water medium was again verified and successfully analyzed by this method.

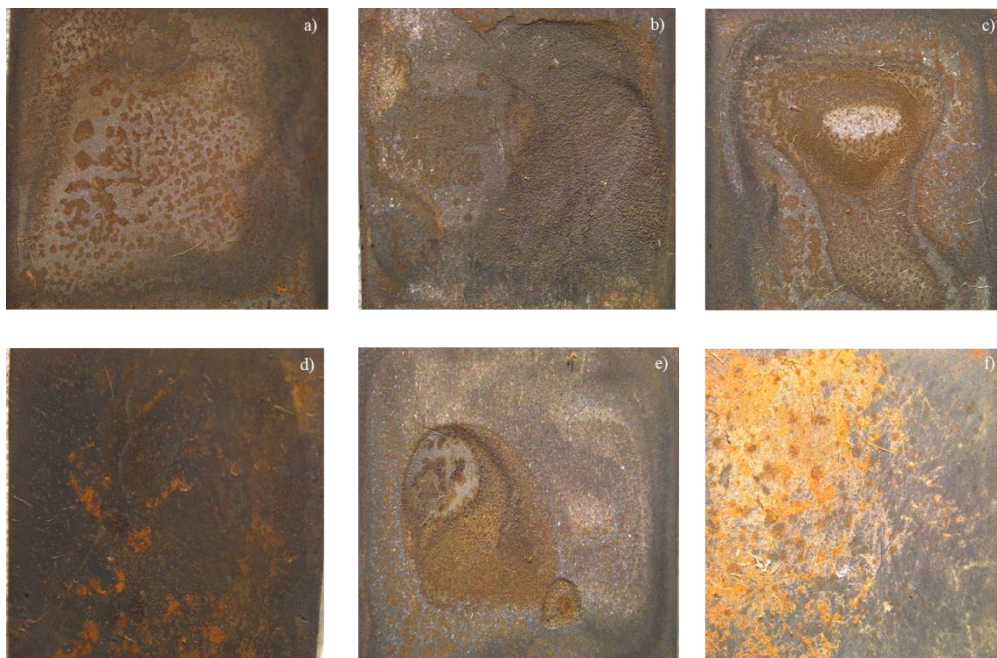


Fig. 9.6: Optical micrographs of mild steel coupons exposed in a) control b) biotic c) NHP2M d) NHP3M e) 2PHEP f) 2TAEP

❖ *UV-Visible spectroscopy*

The mechanism of MIC inhibition can be further interpreted by UV-Visible spectroscopy. The affinity of Schiff base inhibitor towards metal surface can be confirmed by taking UV-Visible spectra of inhibitor and ferric salt solutions individually and combined. Almost all ferrous ions will convert into ferric ions in the artificial sea water medium ($\text{pH}=7.5 \pm 0.5$). So the interaction between Schiff base inhibitor and mild steel metal can be studied by employing the ferric salt solution and inhibitor.

Fig. 9.7 shows UV-Visible spectra of 2PHEP, FeCl_3 and an equal mixture of 2PHEP and FeCl_3 . 2PHEP shows 3 distinct peaks at 407 nm, 316.5 nm and 265.5 nm, which can be attributed to $n \rightarrow \pi^*$ (R-band), $\pi \rightarrow \pi^*$ (benzenoid band) and $\pi \rightarrow \pi^*$ (K band) transitions respectively. After mixing 2PHEP with ferric salt solution, there is a notable difference in absorbance values for the FeCl_3 -2PHEP spectrum from the individual

spectra. The peak at 407 nm due to 2PHEP is shifted to 402.5 nm. The value of absorbance for the FeCl_3 -2PHEP mixture was found to be decreased. This blue shift can be ascribed to the transfer/adsorption of 2PHEP molecules from the medium to the mild steel surface. A significant decrease in intensity observed at 402.5 nm for FeCl_3 -2PHEP mixture clearly show strong binding interaction between 2PHEP molecules and FeCl_3 due to quenching. The substantial changes in the characteristics of the UV-Visible spectra pointed out the possible complexation between Schiff base inhibitor and metal.

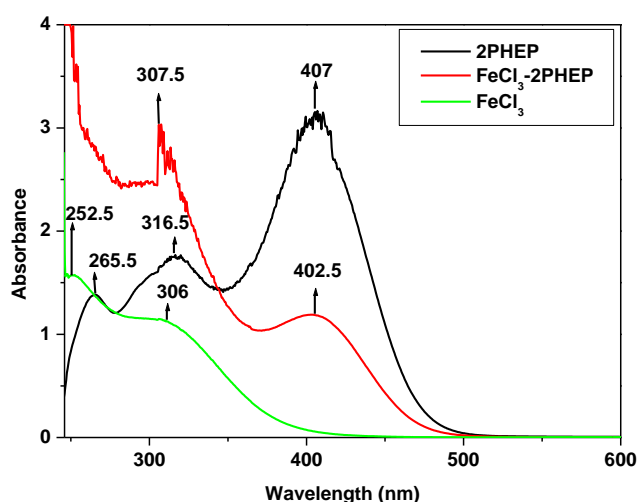


Fig. 9.7: UV-Visible spectra of 2PHEP, FeCl_3 and 1:1 mixture of 2PHEP and FeCl_3

Conclusions

- Schiff base inhibitors derived from pyridine carbaldehyde and acetyl pyridine 1) *N*-hydroxy-1-(pyridin-2-yl)methanimine, NHP2M 2) *N*-hydroxy-1-(pyridin-3-yl)methanimine, NHP3M 3) (E)-2-(1-(2-phenylhydrazono)ethyl)pyridine, 2PHEP and 4) (E)-2-(1-triazylideneethyl)pyridine, 2TAEP were applied as MIC inhibitor on mild steel in the artificial seawater medium.

- All the Schiff base inhibitors showed appreciable inhibition efficiency. The decreasing order of inhibition efficiency of Schiff base inhibitor systems as follows: NHP3M > 2PHEP > NHP2M > 2TAEP.
- Isolation and identification of the resulting culture showed the possibility of mixed culture of related bacteria in the isolate from original seawater.
- Impedance parameters were going along with data obtained in weight loss measurements.
- Shifting of corrosion potential (E_{corr}) for the Schiff base inhibitor system to a positive potential revealed a better corrosion resistance on the metal surface.
- Potentiodynamic polarization studies revealed that Schiff base inhibitors were acted as a mixed-type inhibitor.
- In vitro antibacterial effects of inhibitors showed that the order of antibacterial effect was NHP3M < NHP2M < 2PHEP < 2TAEP. So, the mechanism of inhibition was proposed that Schiff base molecules destabilize biofilm formation by adsorption of Schiff base molecules on the mild steel surface, not by killing the microorganism.
- Proposed mechanism was established by surface analysis like XRD and FTIR of corrosion products. XRD spectrum of metal dipped in the biotic system showed an intense peak of Fe_2O_3 , which represents increased corrosion by the influence of microorganisms. FTIR spectra of corrosion products of inhibitor systems revealed that Schiff bases could act as destabilizing agents for biofilm formation.
- Microscopic surface analysis of metal surfaces exposed in Schiff base inhibitor systems showed the protective nature of inhibitors.

- The affinity of Schiff base inhibitor towards metal surface proved by UV-Visible spectra. Decrease in intensity for FeCl_3 -2PHEP mixture showed strong binding interaction between 2PHEP molecules and FeCl_3 .